A NEW COORDINATE TRANSFORMATION FOR TURBULENT

BOUNDARY LAYER FLOWS

J. E. Carter, D. E. Edwards, and M. J. Werle
United Technologies Research Center
East Hartford, Connecticut

ABSTRACT

A new self adaptive coordinate transformation for the finite-difference solution of turbulent boundary-layer flows is presented which permits a uniform mesh to be used in the computational coordinate which extends across the layer. This coordinate transformation uses the local value of the skin friction coefficient to scale the thickness of the wall layer region, and the local maximum value of turbulent viscosity to scale the boundary-layer thickness. Results are presented for two dimensional boundary layers in both positive and negative pressure gradients and comparisons are made with experimental data and conventional variable-grid results for low-speed turbulent boundary-layers. The cases chosen illustrate the capability of this new transformation to capture the boundary layer growth over the full extent of laminar, transitional, and turbulent flow with no grid adjustment as well as its ability to consistently enlarge the wall layer region for accurate shear stress representation. In addition, preliminary results of mesh refinement studies using the new coordinate transformation are presented.

197

Figure 1. Introduction

Current procedures which are used to generate the mesh across a turbulent boundary layer require the specification of several mesh parameters which are generally difficult to relate to the length scales of the flow itself. In addition, these length scales vary as the solution evolves downstream thereby resulting in a mesh which although "optimum" in one region, may be inappropriate in another. The objective of the present investigation is to develop a procedure which simplifies the specification of the grid point distribution across the turbulent boundary layer. It is desired to have this procedure properly account for the growth of the wall layer as well as the overall boundary-layer thickness. Since most flows are initially laminar at the start of the boundary layer and then are followed by transition to turbulent flows then this procedure should be uniformly applicable to laminar, transitional, and turbulent flows. The approach taken is to develop an adaptive grid technique based on known analytical properties of boundary layer flows. This approach results in a coordinate transformation which is based entirely on fluid dynamic concepts.

Objective

- **Develop a procedure which:**

  - **Simplifies specification of grid point distribution across turbulent boundary layer**

  - **Properly accounts for wall layer and boundary layer thicknesses**

Approach

- **Adaptive grid technique based on known analytical properties of boundary layer flows**

Figure 2.   Grid Requirements for Turbulent Boundary Layers

It is well known that turbulent boundary layers are characterized by two transverse length scales, the boundary layer thickness and the wall layer thickness. These two length scales generally are quite different in magnitude thereby making the analysis of turbulent layers more complicated than laminar boundary layers where generally only one length scale is present, the boundary layer thickness. In addition the wall layer and boundary layer thicknesses vary in the stream direction depending upon the pressure gradient, wall boundary conditions, etc. In laminar flow it has been shown that when the boundary layer equations are expressed in terms of the Levy-Lees variables, the streamwise growth of the boundary layer is significantly reduced thereby simplifying the numerical solution of the governing equations. Most turbulent analyses also use the Levy-Lees variables but since these variables do not properly capture the boundary layer thickness it is necessary to monitor the numerical solution and add points in the outer region to accommodate the boundary layer growth. Also, in order to provide adequate resolution of the wall and wake region and simultaneously use as few grid points as possible, practically all numerical approaches for turbulent boundary layers use a fine mesh near the wall and a coarser mesh in the outer region as shown here. There are two difficulties with this approach: 1) the initial choice of the mesh distribution, and 2) the adjustment of this mesh as the wall and boundary layer thicknesses vary downstream. A new coordinate transformation was devised to simultaneously capture the boundary layer growth and automatically scale the inner wall layer region thereby allowing a uniform step to be used in the transformed coordinate, N. The resulting turbulent profile, schematically shown here, has the appearance of a laminar profile when plotted in terms of N.

Laminar Levy Lees
- **Monitor edge growth**
- **Variable grid to resolve wall layer**

η u

η Boundary layer edge
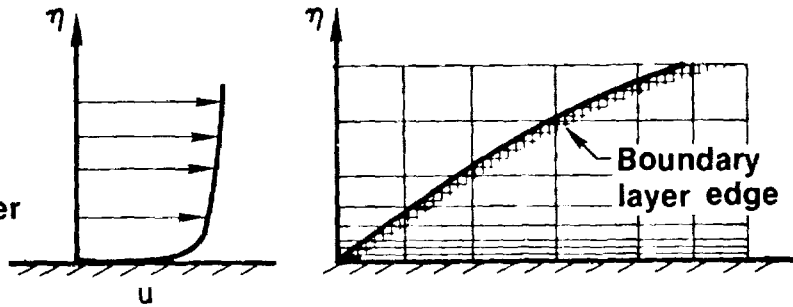
Coordinate transformation
- **Growth capture**
- **Automatic wall layer scaling**
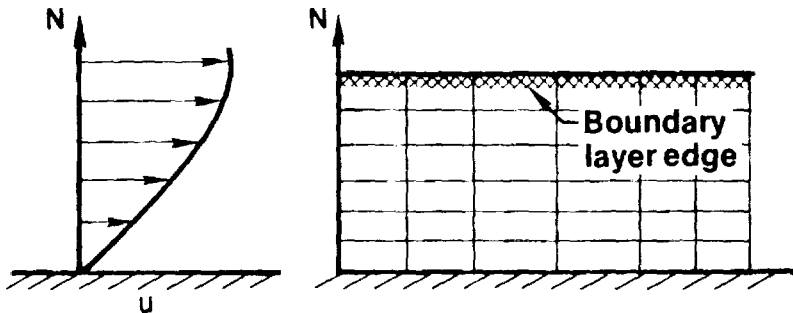
N   u

N   Boundary layer edge

Figure 3.   Capture of Turbulent Boundary Layer Growth

The development of the coordinate transformation begins by first generalizing the Levy-Lees transformation for laminar flow to turbulent flow by using a reference turbulent viscosity level to replace the laminar edge viscosity in these transformed variables. For laminar flows the usual Levy-Lees transformation converts the equations from physical variables to similarity variables such that even when the flow is not self-similar the boundary layer edge is essentially constant in the transformed normal coordinate. In the laminar case the normalized molecular viscosity coefficient is $O(1)$ in the outer region of the boundary layer. For the turbulent case this transformation is modified to normalize the turbulent viscosity coefficient to $O(1)$ in the outer region but is done in such a manner that the form of the equation is unchanged from the laminar set. Thus in these transformed variables, in the outer region, the solution for laminar and turbulent flow should be approximately the same since the outer boundary condition ($F=1$) is the same for both. Therefore, since these variables capture the boundary layer growth in laminar flow, the same growth capture should occur in the turbulent case. The turbulent Levy Lees transformation is a generalization of that used by Schlichting in his Ph.D. thesis in 1930 to transform the turbulent momentum equation for jets and wakes into a "laminar-like" form thereby permitting the laminar similarity solution to be used for a turbulent flow. The new turbulent Levy Lees transformation can be used with any turbulence model provided that a representative turbulent viscosity level can be identified. In the present work the two-layer algebraic eddy viscosity model of Cebeci and Smith was used, in which the reference turbulent viscosity is that for the outer layer. This value varies only with the distance along the surface since an intermittency function was not used at the boundary layer edge.

$$\xi = \int_0^s \rho_e \mu_{t_e} u_e \, ds \qquad \eta = \frac{\rho_e u_e}{\sqrt{2\xi}} \int_0^n \frac{\rho}{\rho_e} \, dn$$

$$\mu_{t_e} = \mu_e \left(1 + \frac{\epsilon}{\mu}\right)_{ref}$$

$\epsilon_{ref} = 0$ **Laminar Levy Lees transformation**

$\epsilon_{ref} \neq 0$ **New turbulent Levy Lees transformation**

$$F = \frac{u}{u_e} \qquad V = \frac{2\xi}{\rho_e \mu_{t_e} u_e} \left(\frac{\rho v}{\sqrt{2\xi}} + F \eta_s\right) \qquad \beta = \frac{2\xi}{u_e} \frac{du_e}{d\xi}$$

Continuity: $2\xi F_\xi + F + V_\eta = 0$

Momentum: $2\xi F F_\xi + V F_\eta = \beta\left(1 - F^2\right) + \left[\frac{\rho \mu_t}{\rho_e \mu_{t_e}} F_\eta\right]_\eta$

where $\mu_t = \mu\left(1 + \frac{\epsilon}{\mu}\right)$

200

Figure 4. Composite Coordinate Transformation

The use of the turbulent Levy Lees transformation avoids the need to continuously add or subtract grid points at the edge of the turbulent boundary layer due to boundary layer growth or decay. However, a variable grid distribution is still required, in fact now even more so, to adequately resolve the wall layer thickness since it has been correspondingly reduced along with the boundary-layer thickness. Clearly, an inner region transformation is needed to enlarge, in the computational coordinate, the high gradient wall region. Fortunately, the analytical behavior of the turbulent boundary layer profile is known in the wall layer region and this information can be used as the basis for an inner region (wall layer) transformation. It has been established numerous times both analytically and experimentally over the past 40 years that the velocity varies with the logarithm of the distance normal to the wall in the wall region. This relationship is not valid in the immediate vicinity of the wall since it is singular and must be replaced with the laminar sublayer profile where the velocity varies linearly with the distance normal to the wall. Hence a logarithmic coordinate transformation could not be used if we want to solve the equations all the way to the wall, which is desired in most boundary-layer analyses. In a recent paper, Whitfield presented a new analytical expression for the velocity profile in the wall region which also has the proper analytical behavior in the laminar sublayer. This analytical expression is used in the present work in the wall or inner region such that a constant increment in the transformed coordinate results in a constant increment in velocity. With the inner region coordinate transformation established it is now necessary to specify a suitable transformation for the outer or wake region. The outer coordinate transformation is motivated by the observation that with the turbulent Levy Lees transformation discussed in figure 3, the boundary layer edge is fixed and the governing equations closely resemble the laminar equations in the outer region. Hence the outer transformation is deduced from a function which closely fits the Blasius solution. Whitfield found that this function closely fits turbulent data in the outer region which supports the idea that in this region the laminar and turbulent solutions resemble each other. A composite transformation is established by combining the inner and outer transformations employing concepts from the method of matched asymptotic expansions. The final result is that the semi-infinite physical space $o \leq y \leq \infty$ is mapped into a unit interval $0 \leq N \leq 1$ in the computational coordinate N, and that the transformation used is based completely on fluid dynamic concepts to assure a universal applicability of the method. A sketch of the inner, outer, and composite functions is shown to illustrate their relative magnitudes.
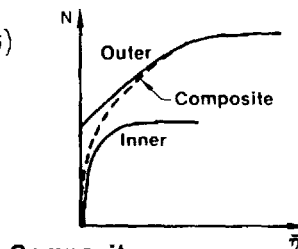
Inner region:

$$N_i \sim \left. \frac{u}{u_e} \right|_i = k_1 \sqrt{C_{f_e}} \, \tan^{-1} \left(k_2 \sqrt{\xi C_{f_e}} \, \bar{\eta} \right)$$

- Analytical solution by Whitfield
- Correct in sublayer, $u^+ = y^+$

Outer region:

$$N_o \sim \left. \frac{u}{u_e} \right|_o = \tanh^{1/2} d \left(\bar{\eta} + \bar{\eta}_0 \right)^2$$

- Normalized viscosity implies outer region is "laminar-like"
- Good fit to Blasius solution
- Found by Whitfield to match experimental data

Composite:

$$N_c = N_i + N_o - N_{i/o}$$

- Matching condition $N_{i/o} = N_{o/i}$
- Solve for $\bar{\eta}_0$

Figure 5. Implement Coordinate Transformation

The composite coordinate transformation presented in figure 4 is incorporated into the boundary-layer equations expressed in terms of the turbulent Levy Lees variables which were discussed in figure 3. The transformed equations are obtained in a straightforward manner and are not substantially different from those in figure 3 other than the explicit dependence of the term $\partial N/\partial \xi$. These equations are solved with a standard implicit finite-difference scheme in which a uniform mesh is used in the normal direction. The use of the coordinate transformation results in less than a 10% increase in computer time over that used by our UTRC computer code which was recently developed using the variable grid finite difference scheme developed by Blottner. This code has been used in the present work to provide calculations for comparison purposes. This new coordinate transformation is an adaptive grid procedure since it relies on two quantities, the local skin friction and the local reference viscosity to complete the specification of the composite coordinate at each stream-wise location. In the results presented here these quantities were obtained from the solution at the previous station since a non-iterative scheme was used. This adaptive grid procedure is applicable to laminar flows since the wall layer region is nonexistent (hence $N_i = 0$) and only the outer transformation is used. In transitional flows the wall layer region is initiated at the start of transition and thus allows for the natural development of the wall region as the flow evolves from a laminar to a turbulent boundary layer.

- **Finite difference solution of equations in ξ, N coordinates**

- **Adaptive grid — C_{f_e} and $\left(1+\frac{\epsilon}{\mu}\right)_{ref}$ depend on local solution**

- **Applies to laminar, transitional, and turbulent flow**

    Laminar — set $N_i = 0$

    Transitional — inclusion of inner region initiated at start of transition

    Turbulent — composite transformation

202

Figure 6. Skin Friction Distribution - Flat Plate

This figure shows a comparison of the skin friction distribution obtained from calculations in which the composite coordinate transformation (adaptive grid) and the variable grid (geometric progression) techniques were used. Both predictions agree well with the experimental data of Wieghardt. In the present case 101 points were used across the layer and there is no plottable difference in the results. Reduction in the number of points from 101 to 21 resulted in essentially the same solution using the adaptive grid; the same reduction for the variable grid scheme resulted in a slightly different solution as shown here. The arrows indicate the locations at which profiles from the different approaches will be compared.

Legend:
- - - - {Adaptive grid, $N = 101,21$
Variable grid, $N = 101$

——— Variable grid, $N = 21$

o Exp. data (Wieghardt)

$Re_\infty/m = 2.2 \times 10^6$

$u_\infty = 33$ m/s

Y-axis: C_{f_e} ranging from 0 to 0.006

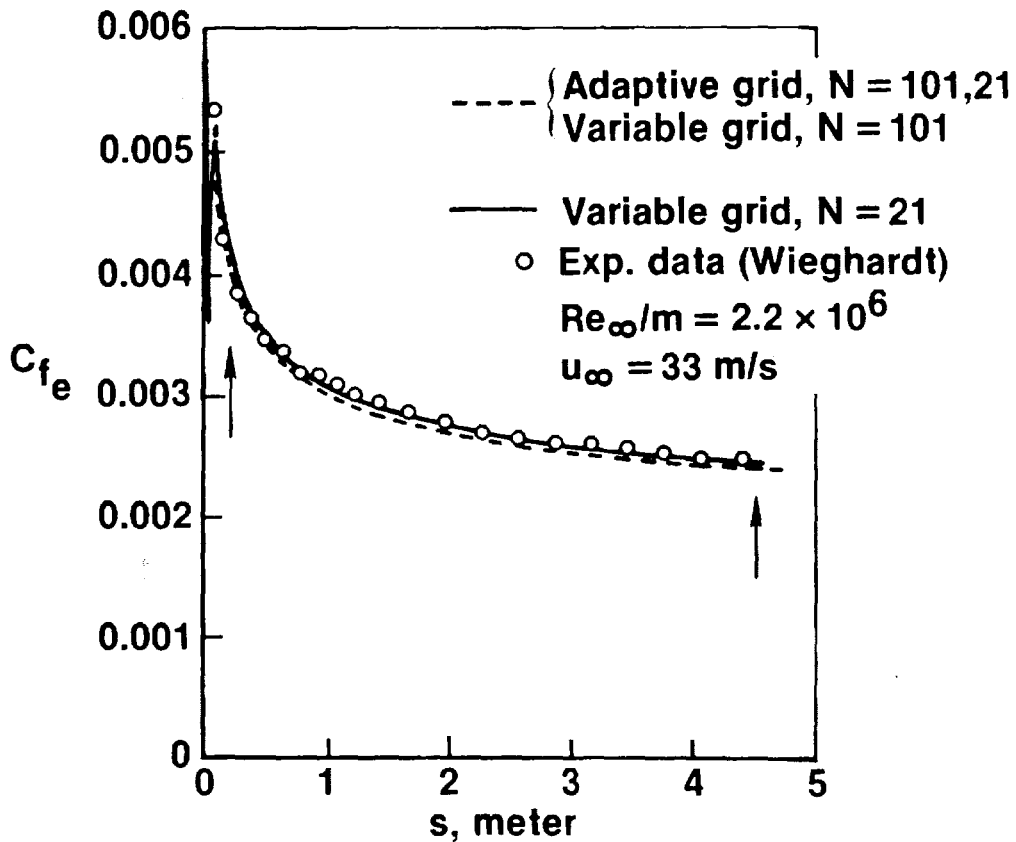X-axis: s, meter ranging from 0 to 5

Figure 7. Displacement Thickness Distribution - Flat Plate

    Shown here is a comparison of the displacement thickness distributions from the
adaptive grid scheme versus that measured experimentally. The agreement is good and
the solution is shown to change only a few percent when the grid is reduced. Similar
changes were found to occur in the variable grid scheme when the same grid reduction
was made. Detailed grid studies are presently underway in order to compare the
relative truncation errors of the adaptive grid scheme and the variable grid scheme.
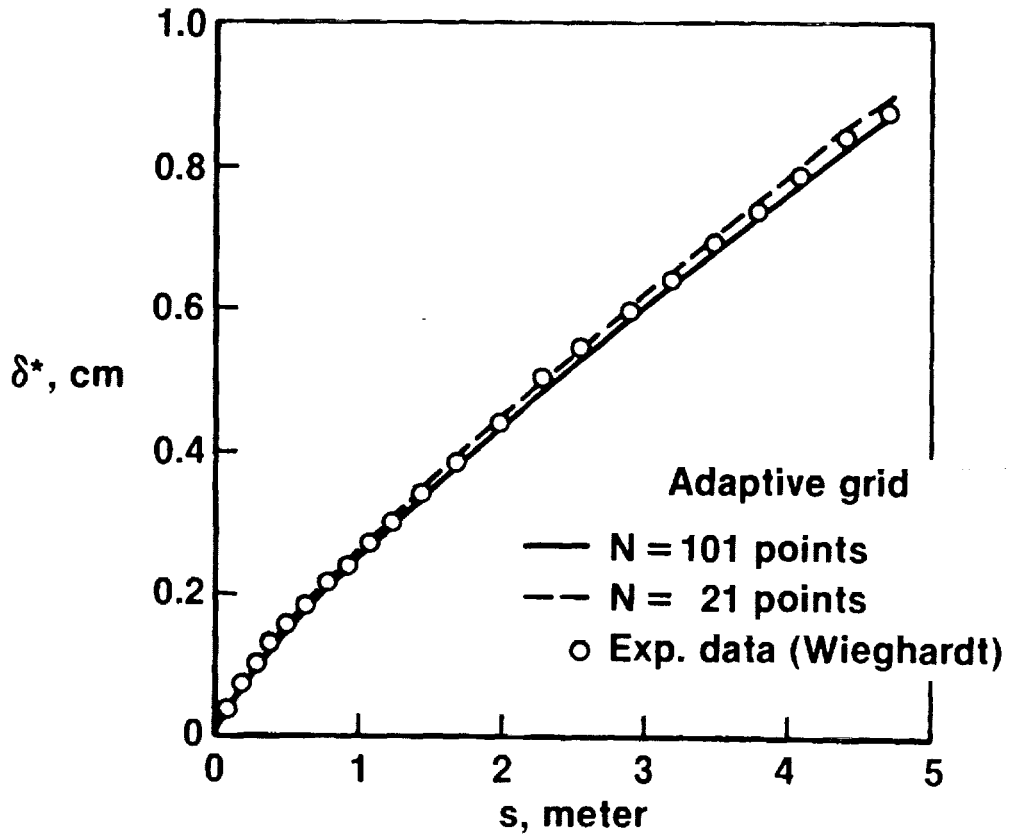
Figure 8. Velocity Profiles in Laminar Levy Lees Variables

In the next several figures flat plate velocity profiles at the locations previously indicated in figure 6 will be shown in terms of the normal coordinate as given by the laminar Levy Lees transformation, the turbulent Levy Lees transformation, and the composite coordinate transformation. The present figure clearly shows the two-layer structure of the turbulent boundary layer as well as the significant boundary layer growth which occurs in this variable. Use of the laminar Levy Lees transformation for turbulent flows is not significantly different than working in the physical or untransformed coordinate. Also plotted is the Blasius solution which is the laminar self-similar solution for a flat plate. Note that the Blasius solution has a much smaller value of η_e at the edge of the boundary layer than the turbulent profiles despite the higher skin friction (slope at wall) in the turbulent case.
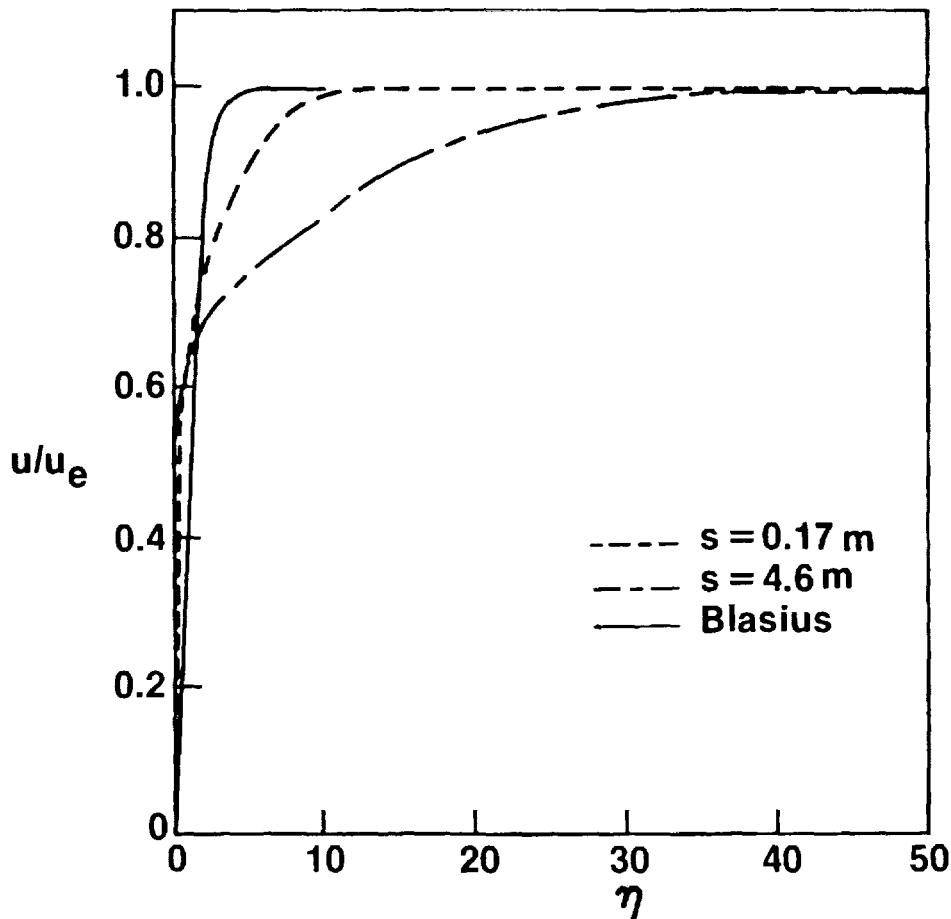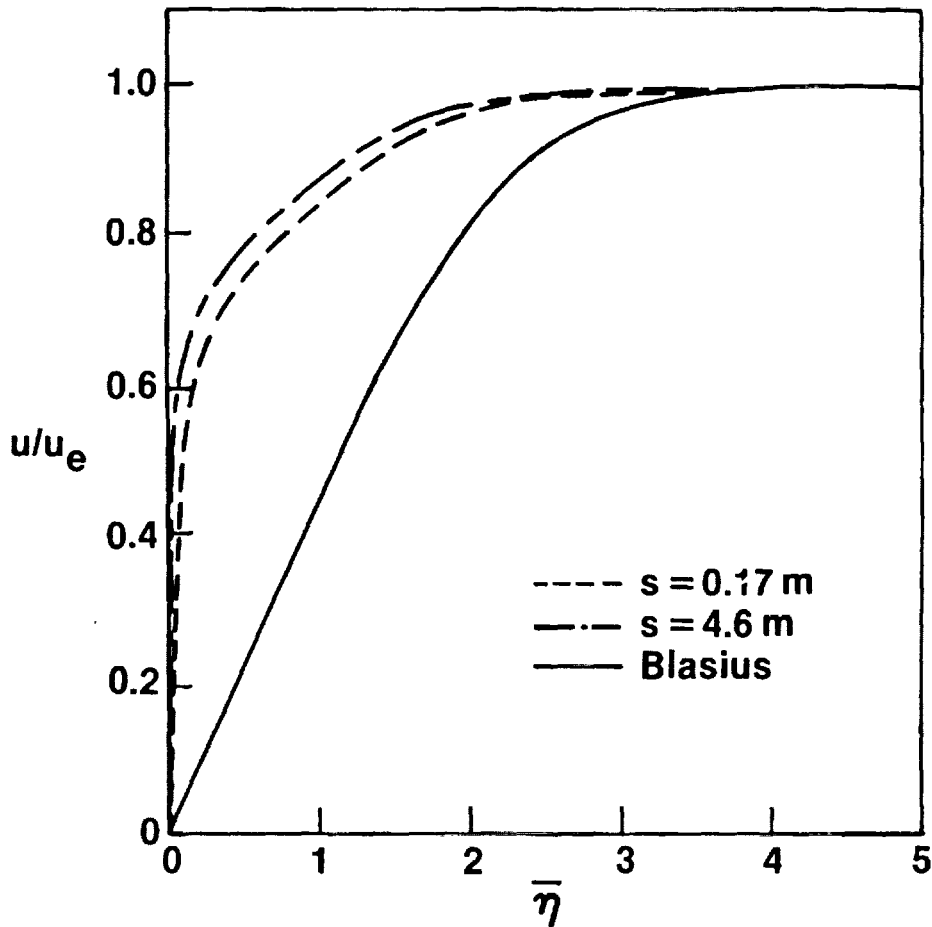

205

Figure 9. Velocity Profiles in Turbulent Levy Lees Variable

This figure shows the same profiles in the new turbulent Levy Lees variable and indicates that the turbulent boundary-layer thickness has been preserved in this new variable and that it is nearly the same value as that of the Blasius profile. The bar over the η-coordinate is used to distinguish between the turbulent Levy Lees variable and the laminar Levy Lees variable as discussed in figure 3. Both variables have the same form; it is only the interpretation of the ξ-variable contained in the η-variable which distinguishes the two transformations. Despite the capture of the turbulent boundary layer growth, it is seen in this figure that the high gradient wall region still persists which requires a variable grid for adequate resolution.

206

Figure 10. Growth of Boundary Layer Thickness - Flat Plate

   This figure shows a comparison between the streamwise variation of the boundary
layer edge as deduced in the laminar Levy Lees variable versus that obtained in
terms of the turbulent Levy Lees variable. The ability of the turbulent Levy Lees
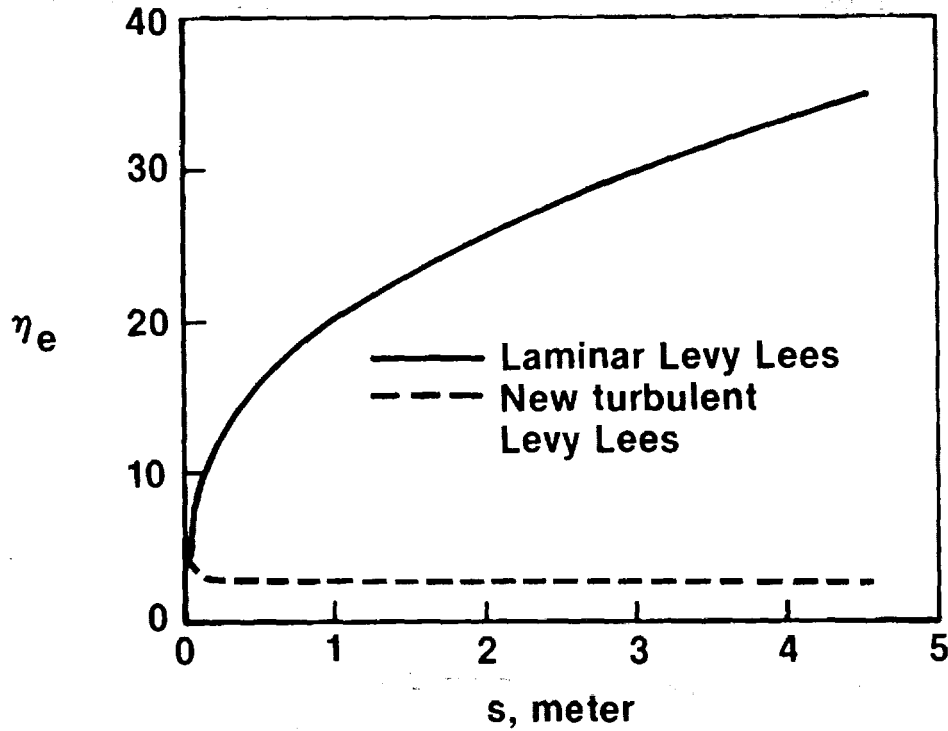variable to capture the turbulent boundary layer growth is clearly seen here.

Figure 11. Velocity Profiles in New Composite Coordinate

This figure presents the same profiles shown previously now plotted in terms of the new composite coordinate. It is seen that this transformation results in an enlargement of the wall region, and since the boundary layer edge is captured by the turbulent Levy Lees transformation, the computed turbulent profiles show the same $O(1)$ variation across the layer as the laminar profile thereby permitting a uniform mesh to be used. It is seen that in terms of this new composite coordinate the turbulent profiles change only slightly over a flat plate distance of 4.5M. These changes are greater in the outer region than they are in the inner which is probably due to the more approximate outer coordinate transformation as compared to the use of Whitfield's analytical solution for the inner transformation.
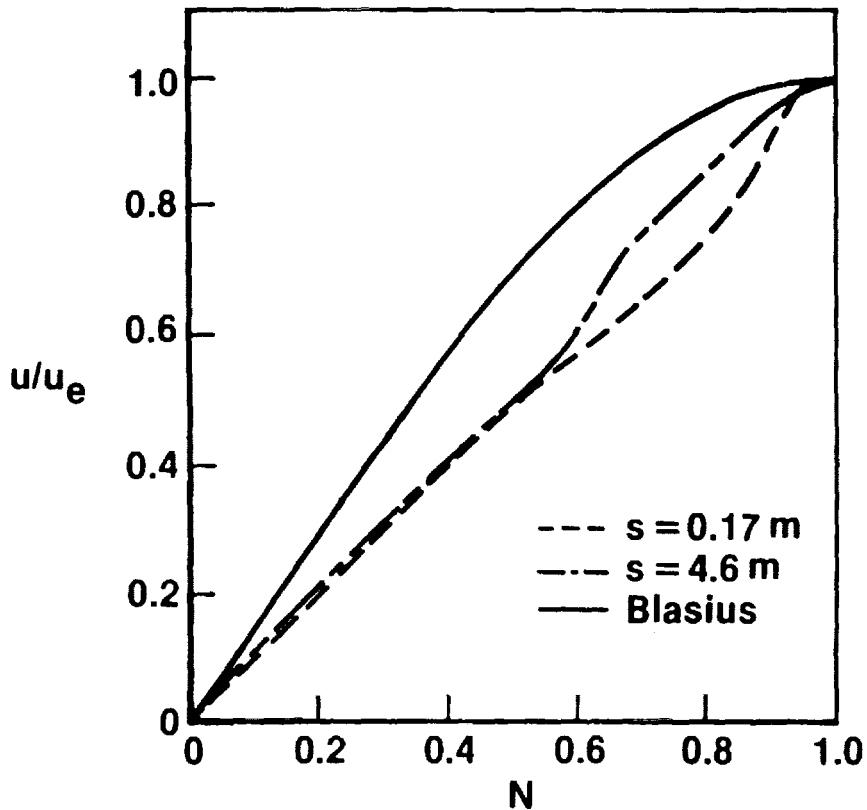
Figure 12. Edge Velocity Distribution

The previous example was a flat plate in which the imposed streamwise pressure gradient is zero. It is well known that boundary layer flows are strongly influenced by the pressure gradient and thus as a test of the new technique presented herein the edge velocity shown in this figure was imposed as a streamwise boundary condition on the boundary layer equations. This distribution was measured by Schubauer and Klebanoff for the airfoil shown here and provides a good test case for the present work since both regions of favorable and adverse pressure gradient are present.
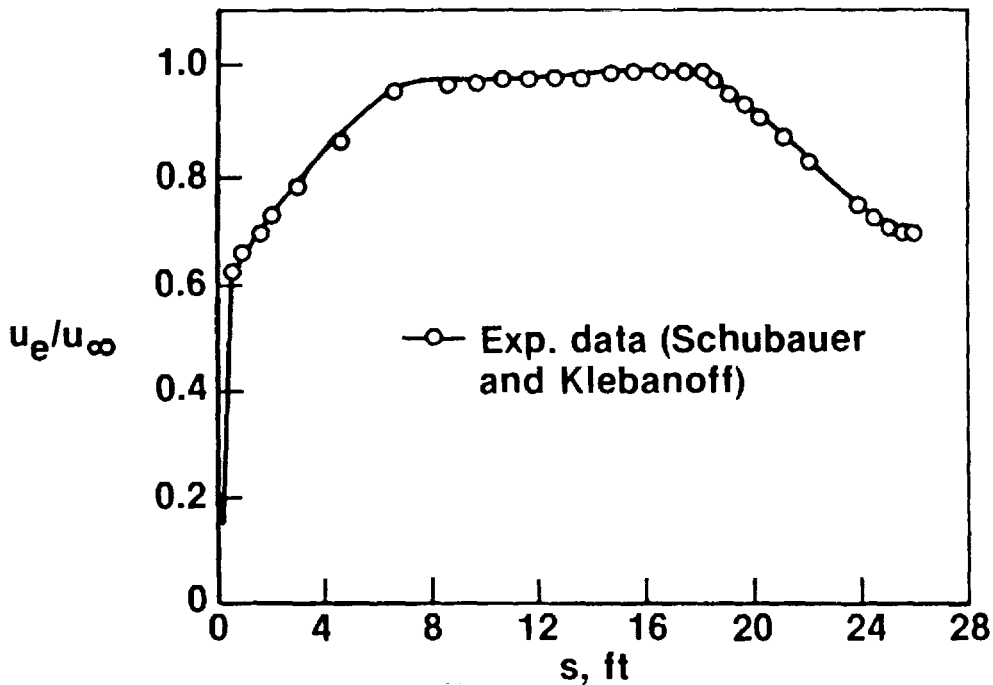
(Note: 1 ft = 0.3048 m)

Figure 13. Skin Friction Distribution - Airfoil

Comparison of the computed skin friction with that measured by Schubauer and Klebanoff is shown here. Excellent agreement is obtained except in the aft strong adverse pressure gradient region where other investigators have concluded that there are three dimensional effects which of course is outside the scope of the present analysis. Comparison of the adaptive grid results with those obtained with the variable grid show that both solutions are the same except in the adverse pressure gradient region where the adaptive grid scheme shows better agreement with the data. Both cases were computed with 101 points across the layer. In the present case the computation does not extend to the separation point so as a further test of the new scheme an analytically imposed edge velocity was prescribed such that separation was encountered. No difficulties were encountered in this case and both the adaptive grid and variable grid schemes yielded nearly the same result.
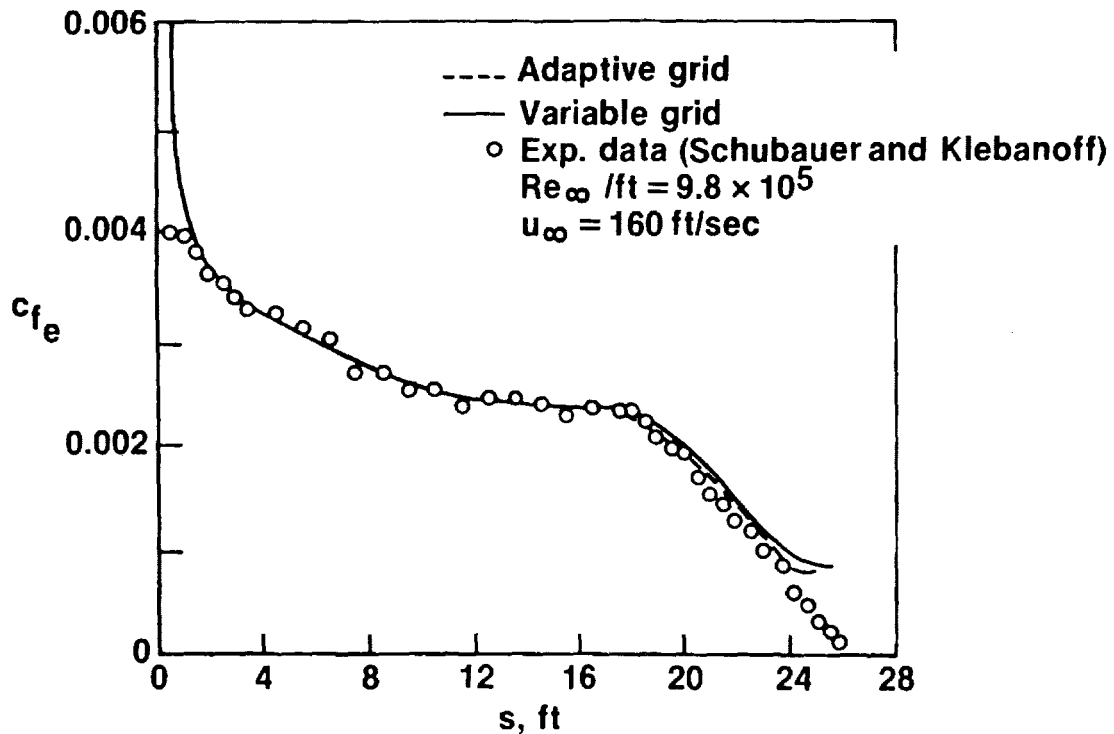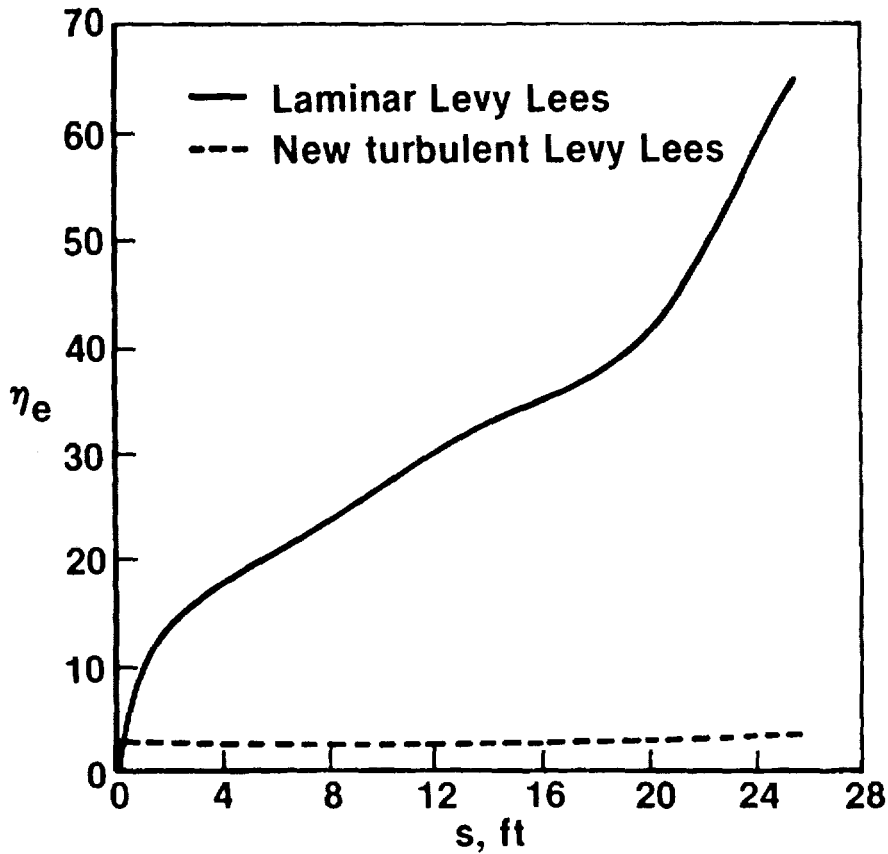

(Note: 1 ft = 0.3048 m)

Figure 14. Growth of Boundary Layer Thickness - Airfoil

This figure shows that the boundary layer edge is captured with the new turbulent
Levy Lees transformation for both positive and negative pressure gradients as was
shown in figure 10 for zero pressure gradient. A slight increase in the boundary-
layer edge is observed with the turbulent Levy Lees transformation in the adverse
pressure gradient region; however, this growth is negligible compared to that which
occurs in the usual laminar Levy Lees variable.

(Note: 1 ft = 0.3048 m)

Figure 15. Conclusions

In conclusion, a new adaptive grid procedure has been presented which automatically captures the boundary layer thickness and simultaneously enlarges the wall layer region through the use of a composite coordinate transformation. This new procedure demonstrates the benefit of using fluid dynamic concepts in mesh generation for numerical solutions since scaling problems and singular regions are properly accounted for. The adaptive grid scheme presented here is simpler to use than a variable grid scheme since now only the total number of desired points needs to be specified by the user. In addition, this adaptive grid procedure has been demonstrated to be applicable to laminar, transitional, and turbulent flows.

- **Adaptive grid procedure automatically captures boundary- and wall-layer thicknesses**

- **New procedure demonstrates benefit of incorporating known analytical properties of the flow into mesh generation**

- **Adaptive grid procedure easier to use than variable grid scheme since only total number of points must be specified**

- **Adaptive grid procedure applies uniformly to laminar, transitional, and turbulent flows**